Adaptive Reference Model Predictive Control for Power Electronics

Yun Yang*, Siew-Chong Tan*
*Department of Electrical and Electronic Engineering
The University of Hong Kong, Hong Kong
Email: sctan@eee.hku.hk

Shu-Yuen (Ron) Hui*†
† Department of Electrical and Electronic Engineering
Imperial College London, U.K.

***Abstract*—An adaptive reference model predictive control (ARMPC) approach is proposed as an alternative means of controlling power converters in response to the issue of steady-state residual errors presented in power converters under the conventional model predictive control (MPC). Differing from other methods of eliminating steady-state errors of MPC based control, such as MPC with integrator, the proposed ARMPC is designed to track the so-called virtual references instead of the actual references. Subsequently, additional tuning is not required for different operating conditions. In this paper, ARMPC is applied to a single-phase full-bridge voltage source inverter (VSI). It is experimentally validated that ARMPC exhibits strength in substantially eliminating the residual errors in environment of model mismatch, load change, and input voltage change, which would otherwise be present under MPC control. Moreover, it is experimentally demonstrated that the proposed ARMPC shows a consistent erasion of steady-state errors, while the MPC with integrator performs inconsistently for different cases of model mismatch after a fixed tuning of the weighting factor.**

Keywords*—Adaptive reference model predictive control (ARMPC); model predictive contro (MPC); steady-state errors; virtual reference; voltage source inverter (VSI); MPC with integrator.

I. INTRODUCTION

Model predictive control (MPC) is a process control in which the future control inputs and system response are predicted at regular intervals with respect to a performance index using a system model [1]. MPC has been found to be well suited for the control of power converters [2]–[13]. In practice, most predictive models are designed based on the so-called nominal model of the power converter, which is a simplified approximated model of the actual power converter since the precise description of the actual model in state-space form is impossible. Besides, power converters may have varying parameters of temperature, operating condition, and lifetime, which are susceptible to external disturbance. This leads to a parametric mismatch between the actual system and the predictive system, which results in the actual system to operate with non-negligible steady-state errors [14] and may violate the required regulation standards. Therefore, it is necessary to compensate the control set such that this error can be mitigated. Several schemes have been proposed to overcome such steady-state errors [10]–[12]. In [10], a Kalman filter is added with MPC to account for unmeasured load variations and to achieve zero steady-state errors. In [11], MPC with long horizons carry the benefits of lowering the total harmonic distortion (THD) of the output as well as reducing the steady-state residues. In [12], MPC with integrator is proposed to reduce the steady-state errors both at the sampling instant and during the intersampling. To integrate the merits of the strategies proposed in [10]–[12] and also extensively simplifying the algorithm, a method that adaptively compensate the control set to mitigate the steady-state errors, which is achieved through the application of trajectory-based control [15]–[18] to the existing framework of MPC, is proposed in this paper. This method is known as adaptive reference model predictive control (ARMPC).

ARMPC has two important components. The first is the virtual references. The predictive strategy in ARMPC exists only to track the virtual references. The other component is the virtual multiple-input-multiple-output (MIMO) system, which derives the virtual references as outputs that are based on the state trajectories in the state plane. The measured change of trajectories reflects the instantaneous status of the system including the variation of the external disturbance or the presence of a model parameter mismatch. The model of the virtual MIMO is flexible. The selection of the algorithm is dependent on the requirement of the output performance and natural properties of the controlled plant. Compared with MPC with Kalman filter, ARMPC can be easily realized by a simple algorithm, using techniques of linear fitting, polynomial fitting, and Gaussian fitting, etc., to achieve the necessary steady-state performance of the system. This enables the implementation of ARMPC using simple micro-controllers. Besides, ARMPC is free of tuning. All the adaptive process is automatically done via measurement and online calculation. This is not the case for the MPC with integrator, which requires tuning of the weighting factor for the integral term. For large-scale nonlinear model mismatch, the system under the control of MPC with integrator has inferior steady-state performance than that under the control of ARMPC.

In this paper, ARMPC is applied to a single-phase full-bridge voltage source inverter (VSI) for illustration. The

advantages of ARMPC over the conventional MPC and MPC with integrator in steady-state performance are experimentally provided. While the illustration of the use of ARMPC in this paper is focused only on the VSI, the proposed ARMPC is widely applicable to all power electronics.

II. Steady-State Issues of MPC

Most previous works on VSI controlled by MPC are limited to current control and *RL* load [4]–[7]. However, for most applications, MPC based on voltage control is more applicable for VSI with *LC* filter (see Fig. 1).

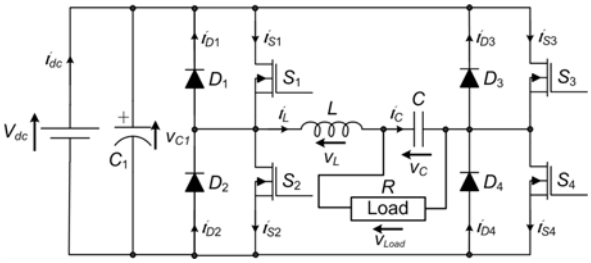

Fig. 1. Single-phase full-bridge inverter with output *LC* filter.

With this, the discrete model of VSI using the Euler's forward method [19] will be

$$\begin{cases} i_L(k+1) = i_L(k) - \dfrac{T_s}{L} v_C(k) + \dfrac{V_{dc} T_s}{L} u(k) \\ v_C(k+1) = \left(1 - \dfrac{T_s}{RC}\right) v_C(k) + \dfrac{T_s}{C} i_L(k) \end{cases}, \quad (1)$$

where T_s is the sampling time, i_L is the inductor current, v_C is the capacitor/load voltage, V_{dc} is the DC input voltage, and u is the control signal. Using the two-step-ahead prediction [11], the predicted voltage at the sampling time $k+2$ for the MPC at the sampling time k is

$$\hat{v}_C(k+2) = \left(1 - \frac{2T_s}{RC} + \frac{T_s^2}{R^2C^2} - \frac{T_s^2}{LC}\right) v_C(k) + \left(\frac{2T_s}{C} - \frac{T_s^2}{RC^2}\right) i_L(k) + \frac{T_s^2 V_{dc}}{LC} u(k). \quad (2)$$

Then, the expression of the cost function can be formulated as

$$J = \underbrace{\Gamma_y \left(v_{\text{ref}}(k+2) - \hat{v}_C(k+2)\right)^2}_{\text{Primary term}} + \underbrace{\Gamma_u \left(u(k) - u(k-1)\right)^2}_{\text{Secondary term}}, \quad (3)$$

where $v_{\text{ref}}(k+2)$ is the actual reference at sampling time $k+2$, and Γ_y and Γ_y are the weighting factors.

Then, the trajectory for tracking the reference can be recovered by solving

$$u^*(k) = \arg\min_{u \in \{-1,0,1\}} J(u), \quad (4)$$

and the corresponding control diagram can be depicted as shown in Fig. 2.

In trajectory-based control, the natural trajectories of a system will ideally correspond to its actual state-space model [15]. If model parameter mismatch exists, the natural trajectories will be changed (see Fig. 3). If the operating trajectory is made to follow a nominal predictive law, the performance of the controlled system will be deteriorated. As shown in Fig. 4(a), when a model mismatch occurs, the state trajectory moves from circle *A* to circle *B*. Fig. 4(b) shows that after the change, the output v_C is incapable of tracking the reference accurately. The results show that under MPC, steady-state errors exist when the model mismatch of the system occurs.

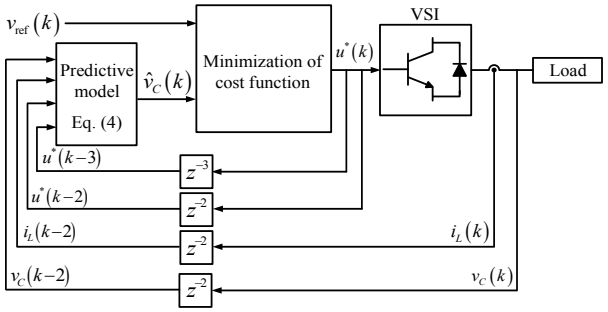

Fig. 2. Model predictive voltage control block diagram of VSI.

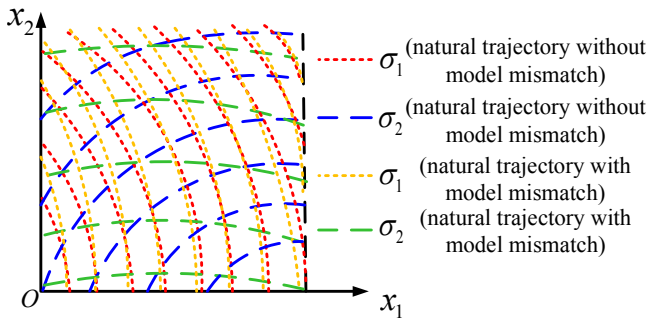

Fig. 3. Model predictive voltage control block diagram of VSI.

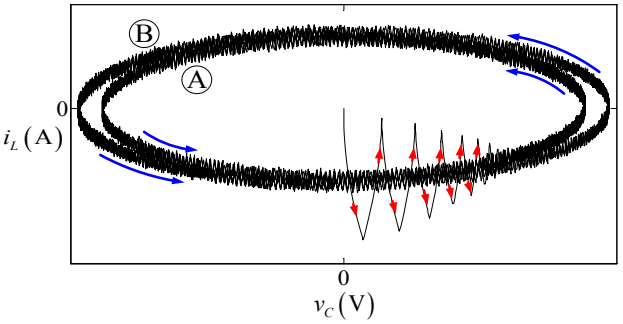

(a) State trajectory

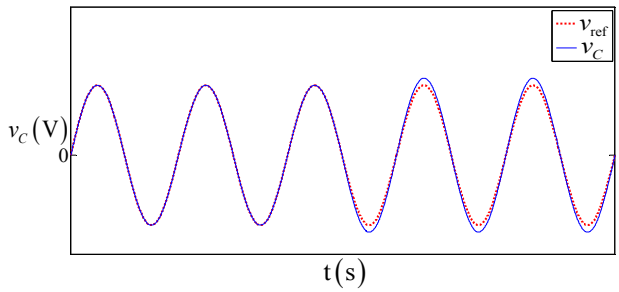

(b) Corresponding output voltage

Fig. 4. State trajectory and the corresponding output voltage of VSI before and after the appearance of model mismatch.

III. PROPOSED ARMPC FOR VSI

Consider the illustration given in Fig. 5 which shows an extreme case where model mismatch exists throughout the entire operation of the VSI. After the appearance of a model mismatch, the root mean square (RMS) value of the output of MPC is shifted from point *A* to *B* to *C* to *D* to *E* and then to *F*. However, if this RMS value can be made to track a set of so-called virtual references y'_{ref1} to y'_{ref1} instead of the actual reference while still based on the nominal state-space model of the system, the steady-state errors in the system controlled by the MPC can be eliminated. Therefore, acquisition of the virtual references is critical in the actualization of ARMPC.

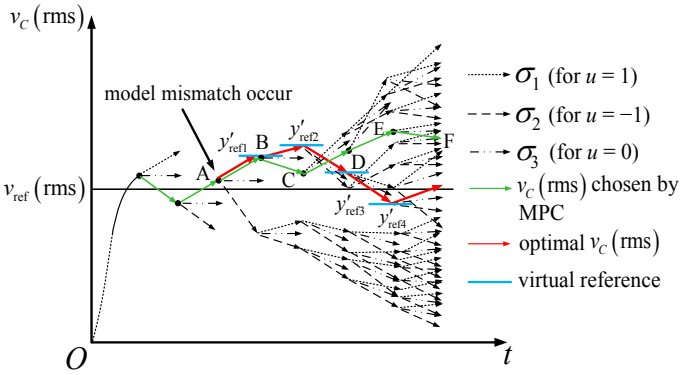

Fig. 5. v_C(rms) and virtual references of the system.

The approach of deriving a virtual MIMO system for generating the virtual references is proposed. The function of the virtual MIMO system can be briefly explained using Fig. 6. Steady-state errors exist between the operating trajectory and the actual reference trajectory. If the virtual reference trajectory *C* inside the actual reference trajectory *A* is tracked, the operating trajectory can be relocated to operate on the actual reference trajectory *A* instead of the trajectory *B*. Conversely (not shown in the figure), if the operating trajectory is located inside the actual reference trajectory, the virtual reference trajectory which is outside the actual reference trajectory will be tracked. Hence, the virtual MIMO system can robustly make the operating trajectory to move in accordance with the actual reference trajectory. In terms of implementation, the virtual MIMO system is built up of a series of past data which can be the positions of the state variables and virtual references.

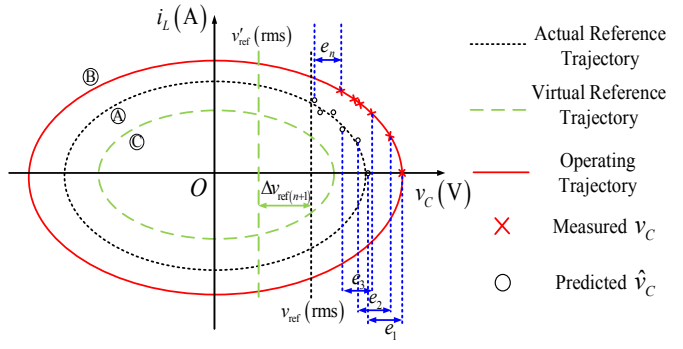

Fig. 6. Virtual MIMO system in the state plane.

For instance, at sampling time *k*, the error between the predicted output voltage $\hat{v}_C(k)$ derived by (2) and the measured output voltage $v_C(k)$ is defined as

$$e(k) = \hat{v}_C(k) - v_C(k), \tag{5}$$

and 2*n* past data of these errors

$$\mathbf{e} = \left[e(k-2n+1), e(k-2n+2), \ldots, e(k)\right] \tag{6}$$

are stored and adopted for the virtual MIMO system. Meanwhile, the corresponding variation of virtual references for the last *n* sampling moment are denoted as

$$\mathbf{\Delta v_{ref}} = \left[\Delta v_{\text{ref}}(k-2n+1), \Delta v_{\text{ref}}(k-2n+2), \ldots, \Delta v_{\text{ref}}(k)\right]. \tag{7}$$

In this paper, considering the scale of the model mismatch in the experiments, the virtual MIMO system is achieve via linear fitting. Then, the virtual MIMO system can be mathematically described as

$$\mathbf{\Delta v_{ref}^T} = \begin{bmatrix} e(k-2n+1) & e(k-2n+2) & \cdots & e(k-n) \\ e(k-2n+2) & e(k-2n+3) & \cdots & e(k-n+1) \\ \vdots & \vdots & \ddots & \vdots \\ e(k-n) & e(k-n+1) & \cdots & e(k-1) \end{bmatrix} \mathbf{K^T}, \tag{8}$$

where $\mathbf{K} = \left[K_1, K_2, \ldots, K_n\right]$ are the weighting factors of the errors on the variation of the virtual references. Due to the number of elements in matrix $\mathbf{\Delta v_{ref}}$ and $\mathbf{K}$ being the same, $\mathbf{K}$ can be derived from (8) as

$$\mathbf{K} = \mathbf{\Delta v_{ref}} \left(\begin{bmatrix} e(k-2n+1) & e(k-2n+2) & \cdots & e(k-n) \\ e(k-2n+2) & e(k-2n+3) & \cdots & e(k-n+1) \\ \vdots & \vdots & \ddots & \vdots \\ e(k-n) & e(k-n+1) & \cdots & e(k-1) \end{bmatrix}^{-1} \right)^{\mathbf{T}}. \tag{9}$$

Then, (9) is applied with $\left[e(k-n+1), e(k-n+2), \ldots, e(k)\right]$ to obtain the variation of the virtual reference $\Delta v_{\text{ref}}(k+1)$ at sampling time *k+1* as

$$\Delta v_{\text{ref}}(k+1) = \mathbf{K}\left[e(k-n+1), e(k-n+2), \ldots, e(k)\right]^{\mathbf{T}}. \tag{10}$$

Then, $\Delta v_{\text{ref}}(k-2n+1)$ in matrix $\mathbf{\Delta v_{ref}}$ in (8) and the first row of the error matrix $\left[e(k-2n+1), e(k-2n+2), \ldots, e(k-n)\right]$ are replaced by $\Delta v_{\text{ref}}(k+1)$ and $\left[e(k-n+1), e(k-n+2), \ldots, e(k)\right]$ respectively to derive a new value of $\mathbf{K}$ for the next iteration. This rolling process will instantaneously gain the information of model mismatch of the system and produce variation of the virtual references in real time. The flowchart of the algorithm for the VSI with ARMPC is shown in Fig. 7.

IV. EXPERIMENTAL VERIFICATION AND DISCUSSION

The experiment is conducted on a Texas Instruments' C2000™ Solar DC/AC VSI. The control used is Texas

Instruments' digital signal processor (DSP) F28069 Piccolo controlCARD. The DC power supply is California Instruments' programmable source CSW5550. The specifications of the VSI are given in Table I. All the values of dominant components are provided by the TI Company, which can be found in the datasheets [20]. The loads used are three incandescent bulbs, at nominal power of 20 W and nominal voltage of 110 V. The number of the stored data $\mathbf{\Delta v}_{\mathbf{ref}}$ for the virtual MIMO system is 3.

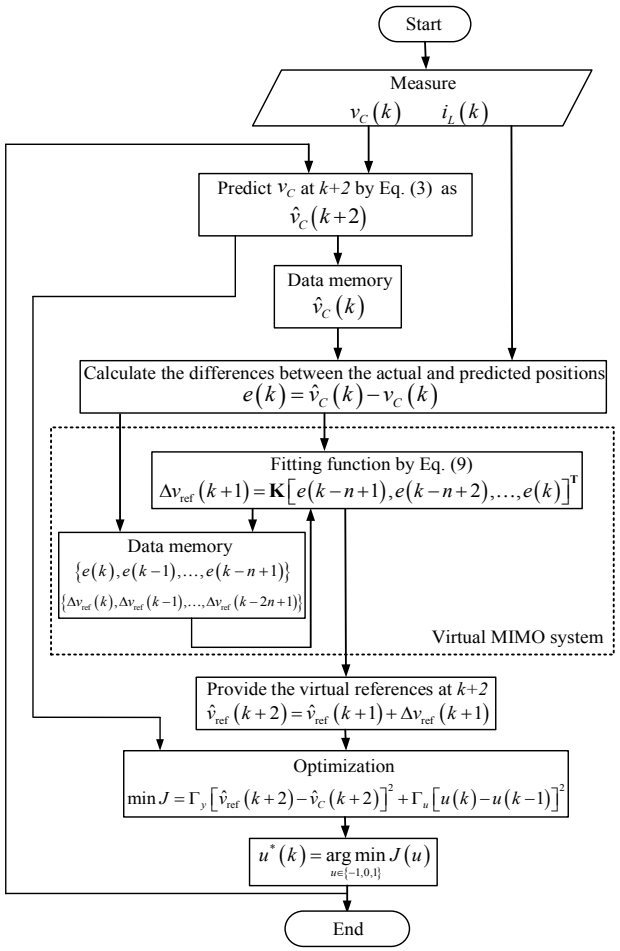

Fig. 7. Flowchart of ARMPC for the VSI.

TABLE I. SPECIFICATIONS OF THE NOMINAL MODEL OF VSI

Parameters	Values	Parameters	Values
V_{dc}	165 V	C_1	470 μF
C	1 μF	L	7 mH
v_{ref} (RMS)	110 V		

The VSI is initially controlled by the MPC with the nominal model. Fig. 8(a) shows the RMS value of v_C to be around 106 V at steady state, which is a 3.64% deviation from the reference when VSI is controlled by MPC. However, when controlled by ARMPC, the steady-state RMS value of v_C is about 110.04 V, which is 0.04% deviation from the reference. In reality, model mismatch exists between the nominal model based on the specifications of VSI provided by datasheet and the actual VSI. If a controller employing the MPC is still designed based on the nominal model, steady-state errors will exist. If ARMPC is adopted, the steady-state errors caused by the model mismatch are eliminated. Meanwhile, the MPC with integrator being proposed in [12] is adopted with a proper tuning of K_i=0.25. The steady-state residuals are nearly removed as shown in Fig. 8(c).

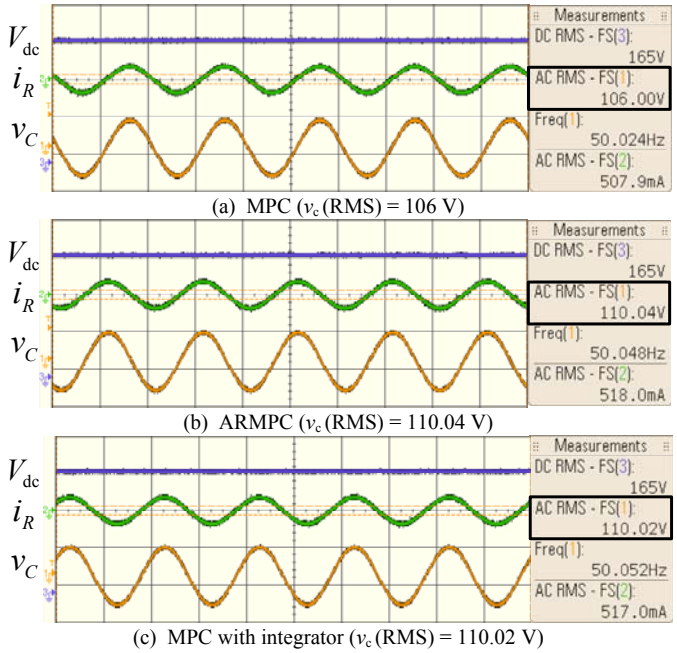

(a) MPC (v_c (RMS) = 106 V)

(b) ARMPC (v_c (RMS) = 110.04 V)

(c) MPC with integrator (v_c (RMS) = 110.02 V)

Fig. 8. Steady-state performance of VSI controlled by (a) MPC, (b) ARMPC, and (c) MPC with integrator based on the nominal model.

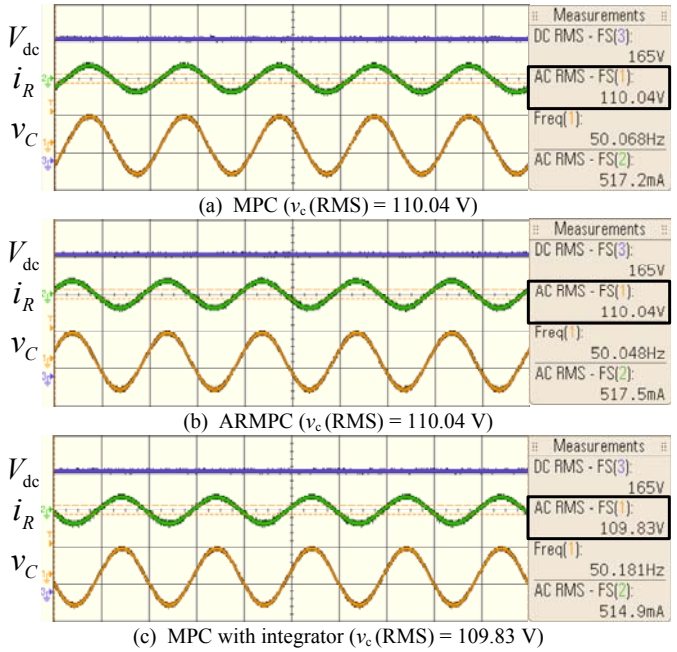

(a) MPC (v_c (RMS) = 110.04 V)

(b) ARMPC (v_c (RMS) = 110.04 V)

(c) MPC with integrator (v_c (RMS) = 109.83 V)

Fig. 9. Steady-state performance of VSI controlled by (a) MPC, (b) ARMPC, and (c) MPC with integrator based on the optimal model.

On the other hand, it is possible to tune by trail-and-error (since precise model is unavailable), an optimal predictive model for MPC and the results of the VSI controlled by MPC based on the optimal model can be obtained as shown in Fig.

9(a). Apparently, MPC with the optimal model has an excellent regulation performance and the RMS value of v_c is about 110.04 V at steady state, which is about 0.04% deviation from the reference. Meanwhile, the VSI controlled by ARMPC and MPC with integrator using the same optimal model can also have an equivalently good performance with the RMS value of v_c being 110.04 V and 109.83 V at steady state, which is about 0.04 % and 0.15 % deviation from the reference, as can be seen in Fig. 9(b) and Fig. 9(c), respectively.

Then, assume that one bulb is burnt out. So, one 20 W bulb is removed, leaving only two 20 W bulbs as loads. Even with the optimal model, the RMS value of v_c is about 112.51 V at steady state, which is 2.28 % deviation from the reference when VSI is controlled by MPC, as can be seen in Fig. 10(a). However, the RMS value of v_c is about 110.06 V at steady state, which is about 0.05 % deviation from the reference when VSI is controlled by ARMPC with the optimal model, as shown in Fig. 10(b). Fig. 10(c) presents the steady-state RMS value of v_c is 108.84 V under the control of MPC with integrator, which is about 1.05 % deviation from the reference, being slightly larger than the deviation of ARMPC.

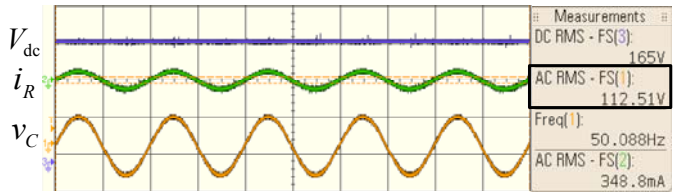

(a) MPC (v_c (RMS) = 112.51 V)

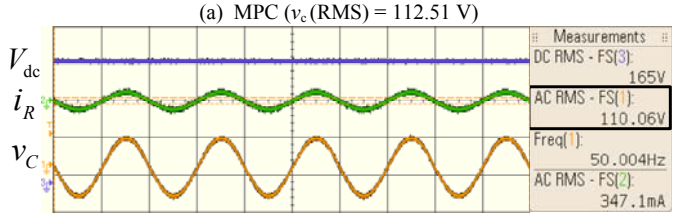

(b) ARMPC (v_c (RMS) = 110.06 V)

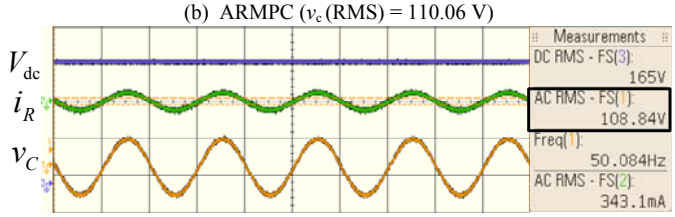

(c) MPC with integrator (v_c (RMS) = 108.84 V)

Fig. 10. Steady-state performance of VSI with a lighter load (two bulbs) controlled by (a) MPC, (b) ARMPC, and (c) MPC with integrator based on the optimal model.

The comparisons of steady-state performance of VSI when the load changes from three 20 W bulbs to one 20 W bulb between MPC, ARMPC, and MPC with integrator are also conducted (waveforms are not shown in the paper). With the optimal model, the RMS value of v_c is about 113.09 V at steady state, which is 2.81 % deviation from the reference when VSI is controlled by MPC. However, the RMS value of v_c is about 110.06 V at steady state, which is about 0.05 % deviation from the reference when VSI is controlled by ARMPC with the optimal model. As for the MPC with integrator, the RMS value of v_c is 1.67 % deviation from the reference. Obviously, VSI being controlled by ARMPC has better steady-state performance than VSI being controlled by MPC and MPC with integrator. MPC with integrator with a selected tuning K_i = 0.25 can guarantee one optimal operating condition to have almost zero steady-state error, but gradually lost its advantage over the conventional MPC when the operation is shifted far away from the optimal operating point. Hence, ARMPC can be perceived as a type of auto-tuning MPC with integrator, which achieves almost zero steady-state error of VSI over a wide operating range.

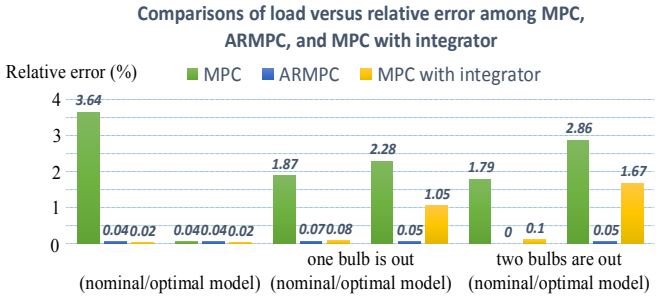

Fig. 11. Comparative bar-charts of the load versus relative error of v_c between the VSI controlled by MPC, ARMPC, and MPC with integrator based on both optimal and nominal models.

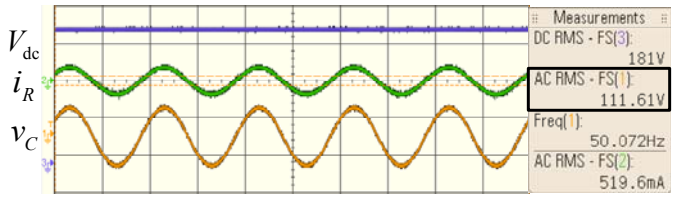

(a) MPC (v_c (RMS) = 111.61 V)

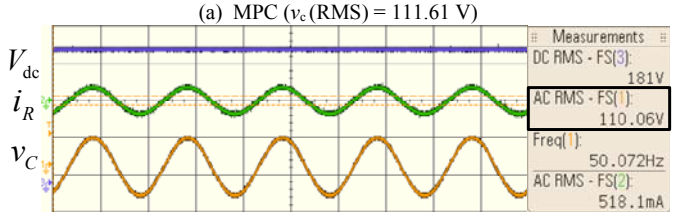

(b) ARMPC (v_c (RMS) = 110.06 V)

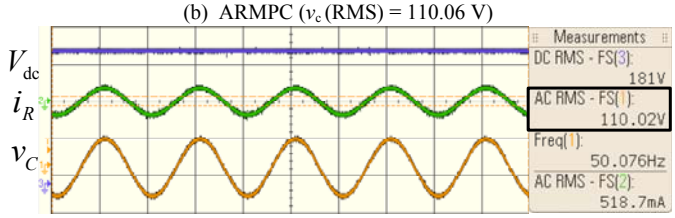

(c) MPC with integrator (v_c (RMS) = 110.02 V)

Fig. 12. Steady-state performance of VSI with V_{dc} change (165 V to 180 V) controlled by (a) MPC, (b) ARMPC, and (c) MPC with integrator based on the optimal model.

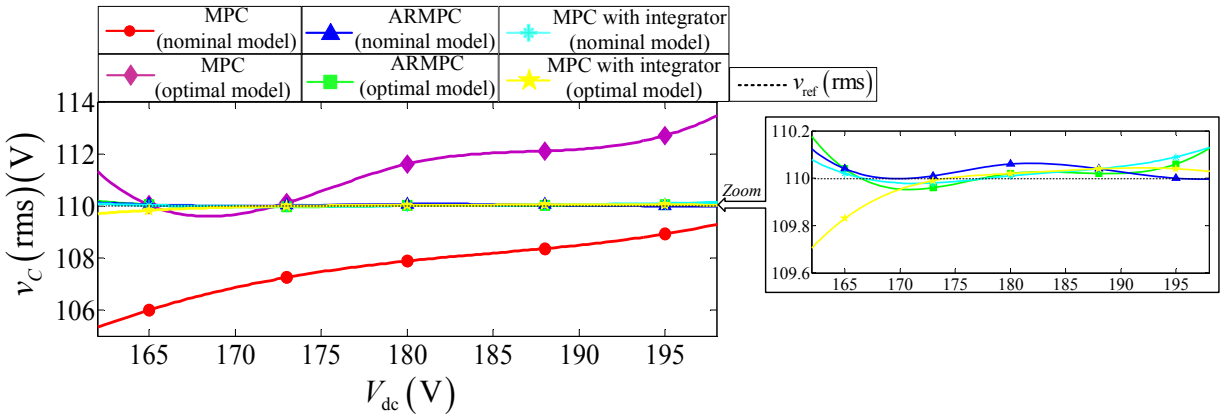

Fig. 13. Comparative curves of V_{dc} versus v_c(RMS) between the VSI controlled by MPC, ARMPC, and MPC with integrator with both optimal and nominal model.

TABLE II. COMPREHENSIVE COMPARISONS OF VC(RMS) BETWEEN MPC, ARMPC, AND MPC WITH INTEGRATOR

Case	MPC	Error	ARMPC	Error	MPC with integrator	Error
Nominal model	106. 00 V	**3.64 %**	110.04 V	**0.04 %**	110.02 V	**0.02 %**
Optimal model	110. 04 V	**0.04 %**	110. 04 V	**0.04 %**	109. 83 V	**0.02 %**
One bulb is out (optimal model)	112. 51 V	**2.28 %**	110. 06 V	**0.05 %**	108. 84 V	**1.05 %**
Two bulbs are out (optimal model)	113. 15 V	**2.86 %**	110. 06 V	**0.05 %**	108. 16 V	**1.67 %**
One bulb is out (nominal model)	107. 94 V	**1.87 %**	110. 08 V	**0.07 %**	109.17 V	**0.08 %**
Two bulbs are out (nominal model)	108. 03 V	**1.79 %**	109. 99 V	**0.00 %**	108. 93 V	**0.10 %**
V_{dc} is changed to 173 V (optimal model)	110. 12 V	**0.11 %**	110. 01 V	**0.01 %**	109. 99 V	**0.00 %**
V_{dc} is changed to 180 V (optimal model)	111. 61 V	**1.46 %**	110. 06 V	**0.05 %**	110. 02 V	**0.02 %**
V_{dc} is changed to 188 V (optimal model)	112. 11 V	**1.92 %**	110. 04 V	**0.04 %**	110. 04 V	**0.04 %**
V_{dc} is changed to 195 V (optimal model)	112. 70 V	**2.45 %**	110. 00 V	**0.00 %**	110. 04 V	**0.04 %**
V_{dc} is changed to 173 V (nominal model)	107. 25 V	**2.50 %**	109. 96 V	**0.04 %**	109. 98 V	**0.02 %**
V_{dc} is changed to 180 V (nominal model)	107. 88 V	**1.93 %**	110. 02 V	**0.02 %**	110. 01 V	**0.01 %**
V_{dc} is changed to 188 V (nominal model)	108. 36 V	**1.49 %**	110. 02 V	**0.02 %**	110. 04 V	**0.04 %**
V_{dc} is changed to 195 V (nominal model)	108. 92 V	**0.98 %**	110. 06 V	**0.06 %**	110. 09 V	**0.08 %**

Additional verification for the conclusions made can also be found in the comparative results of the load change (one bulb out and two bulbs out) by MPC, ARMPC, and MPC with integrator based on the nominal model. To clearly identify the differences between three controllers, a bar-chart based comparison is given in Fig. 11. Apparently, the VSI controlled by ARMPC will always have a better steady-state performance than the VSI controlled by MPC and MPC with integrator when the load deviates from the nominal value. More importantly, it is shown that ARMPC is highly tolerant to parameter shifts and the model it adopts in this situation does not affect its steady-state control performance.

Then, experiments are performed on the VSI based on the change of V_{dc} to study the effect of input voltage change on the output control performance. First, V_{dc} is changed from 165 V to 180 V. Fig. 12(a) shows that with the optimal model, the RMS value of v_c with MPC with 180 V input is about 111.61 V at steady state, which is a 1.46 % deviation from the reference when VSI is controlled by MPC at 165 V. However, in Fig. 12(b), the RMS value of v_c is about 110.06 V at steady state, which is about 0.05 % deviation from the reference when VSI is controlled by ARMPC. In Fig. 12(c), when VSI is regulated by MPC with integrator, the steady-state error is also nearly 0.02 % deviation from the reference. Apparently, VSI controlled by ARMPC and MPC with integrator having better steady-state performance than VSI being controlled by MPC is once again verified. Besides, note that MPC with integrator possess comparable off-set compensation ability to ARMPC for the change of V_{dc}. Then, several values of V_{dc} changing from 165 V to 195 V at 5 V intervals are used for the same experiment.

The curves are shown in Fig. 13. As shown, the VSI controlled by ARMPC will always have a better stead-state performance than the VSI controlled by MPC when the input

voltage changes. Besides, the performance of ARMPC is unaffected by the model used. Meanwhile, MPC with integrator also performs well at steady state when the input voltage is varied.

Table II gives a comparison of the RMS value of the output voltage v_c(RMS) of the VSI with MPC, ARMPC, and MPC with integrator for all different cases. Except for the optimal model case where both MPC and ARMPC have a relative error of 0.04 %, almost all the other cases for MPC have a relative error of greater than 1 % with the largest error being 3.64 %. For ARMPC, all errors are kept within 0.1 %. MPC with integrator is also capable of regulating the relative error within 0.1 % when the input voltage fluctuates, but a load change will deteriorate its steady-state performance to a maximum of 1 %.

V. Conclusions

It has been explained that the method of model predictive control (MPC) applied for controlling power converters will induce non-negligible steady-state errors of the controlled outputs when there is model mismatch. Therefore, various methods, such as MPC with Kalman filter and MPC with integrator have been applied to eliminate the steady-state residues. In this paper, an alternative approach, known as adaptive reference model predictive control (ARMPC) that is based on the trajectory-based control theory and built upon the framework of MPC, is proposed as an alternative means of controlling power electronics of such nature. Instead of tracking the actual references, ARMPC is designed to track the so-called virtual references. As compared with conventional methods, particularly MPC with Kalman filter, the proposed ARMPC can be easily implemented by a low-performance inexpensive digital controller. As an illustration, the proposed ARMPC has been applied to a single-phase full-bridge voltage source inverter (VSI). The experimental results show that the ARMPC will always give a better steady-state performance than the MPC when there exists a model mismatch, load change, and input voltage change. Besides, as compared with MPC with integrator, ARMPC is free of tuning and operates efficiently over a wider operating range.

References

[1] E. F. Camacho and C. Bordons, *Model Predictive Control*, Springer Verlag, 1999.

[2] S. Kouro, P. Cortés, R. Vargas, U. Ammann, and J. Rodríguez, "Model predictive control – a simple and powerful method to control power converters," *IEEE Trans. Ind. Electron.*, vol. 56, no. 6, pp. 1826-1838, June 2009.

[3] J. B. Rawlings and D. Q. Mayne, *Model Predictive Control: Theory and Design*, Nob Hill Publishing, 2009.

[4] J. Rodríguez, J. Pontt, C. A. Silva et al., "Predictive current control of a voltage source inverter," *IEEE Trans. Ind. Electron.*, vol. 54, no. 1, pp. 495-503, Feb. 2007.

[5] P. Cortés, J. Rodríguez, D. E. Quevedo, and C. Silva, "Predictive current control strategy with imposed load current spectrum," *IEEE Trans. Power Electron.*, vol. 23, no. 2, pp. 612-618, Mar. 2008.

[6] R. Vargas, J. Rodríguez, U. Ammann, and P. Wheeler, "Predictive current control of an induction machine fed by a matrix converter with reactive power control," *IEEE Trans. Ind. Electron.*, vol. 55, no. 12, pp. 4362-4371, Dec. 2008.

[7] R. Vargas, P. Cortés, U. Ammann, J. Rodríguez, and J. Pontt, "Predictive control of a three-phase neutral-point-clamped inverter," *IEEE Trans. Ind. Electron.*, vol. 54, no. 5, pp. 2697-2705, Oct. 2007.

[8] P. Cortés, G. Ortiz, J. I. Yuz et al., "Model predictive control of an inverter with output LC filter for UPS applications," *IEEE Trans. Ind. Electron.*, vol. 56, no. 6, pp. 1857-1883, June 2009.

[9] C. E. Garcia, D. M. Prett, and M. Morari, "Model predictive control: theory and practice – a survey," *Automatica*, vol. 25, no. 3, pp. 335-348, May 1989.

[10] T. Geyer, G. Papafotiou, R. Frasca, and M. Morari, "Constrained optimal control of the step-down dc-dc converter," *IEEE Trans. Ind. Electron.*, vol. 23, no. 5, pp. 2454-2464, Sept. 2008.

[11] T. Geyer, P. Karamanakos, and R. Kennel, "On the benefit of long-horizon direct model predictive control for drives with LC filters" in *Energy Conversion Congress and Exposition (ECCE)*, 2014, pp. 3520-3527.

[12] R. P. Aquilera, P. Lezana, and D. E. Quevedo, "Finite-control-set model predictive control with improved steady-state performance," *IEEE Trans. Ind. Inform.*, vol. 9, no. 2, pp. 658-667, May 2013.

[13] T. Geyer, D. E. Quevedo, "Performance of multistep finite control set model predictive control for power electronics", *IEEE Tran. Power Electron.*, vol. 30, no. 3, pp. 1633-1644, Mar. 2015.

[14] J. Rodríguez and P. Cortés, Predictive Control of Power Converters and Electrical Drives, NJ: Wiley, 2012.

[15] P. T. Krein, *Elements of Power Electronics*, Oxford: Oxford University Press, 1998.

[16] K. W. Chan, H. S. Chung, and S. Y. (Ron) Hui, "A genearalized theory of boundary control for single-phase multiplevel inverter using second-order switching surface," *IEEE Tran. Power Electron.*, vol. 24, no. 10, pp. 2298-2313, Oct. 2009.

[17] S. C. Tan, Y. M. Lai, and C. K. Tse, *Sliding Mode Control of Switching Power Converters – Techniques and Implementation*, Boca Raton: CRC, 2012.

[18] M. Ordonez, M. T. Iqbal, and J. E. Quaicoe, "Selection of a curved switching surface for buck converters," *IEEE Tran. Power Electron.*, vol. 21, no. 4, pp. 1148-1153, Jul. 2006.

[19] H. Abu-Rub, J. Guziniski, Z. Krzeminski, and H. Toliyat, "Predictive current control of voltage-source inverter," *IEEE Trans. Ind. Electron*, vol. 51, no. 3, pp. 585-593, June 2004.

[20] "C2000 solar DC/AC single phase inverter schematic," Texas Instruments, USA, 17 Jun. 2014.